

# Fetal Metabolic Stress Disrupts Immune Homeostasis and Induces Proinflammatory Responses in Human Immunodeficiency Virus Type 1– and Combination Antiretroviral Therapy–Exposed Infants

Johannes C. Schoeman,<sup>1</sup> Gontse P. Moutloatse,<sup>2</sup> Amy C. Harms,<sup>1</sup> Rob J. Vreeken,<sup>1,a</sup> Henriette J. Scherpbier,<sup>3</sup> Liesbeth Van Leeuwen,<sup>4</sup> Taco W. Kuijpers,<sup>3</sup> Carools J. Reinecke,<sup>2</sup> Ruud Berger,<sup>1</sup> Thomas Hankemeier,<sup>1,b</sup> and Madeleine J. Bunders<sup>5,6,7,b</sup>

<sup>1</sup>Department of Analytical Biosciences, Leiden Academic Center for Drug Research, Leiden University, The Netherlands; <sup>2</sup>Centre for Human Metabolomics, Faculty of Natural Sciences, North-West University, Potchefstroom, South Africa; <sup>3</sup>Department of Pediatric Hematology, Immunology and Infectious Diseases, Emma Children's Hospital, <sup>4</sup>Department of Gynecology and Obstetrics, <sup>5</sup>Department of Experimental Immunology, and <sup>6</sup>Emma Children's Hospital, Academic Medical Center, University of Amsterdam, The Netherlands; and <sup>7</sup>Research Unit Virus Immunology, Heinrich-Pette-Institute, Hamburg, Germany

Increased morbidity and fetal growth restriction are reported in uninfected children born to human immunodeficiency virus type 1 (HIV-1)–infected women treated with antiretroviral (ARV) therapy. Viruses and/or pharmacological interventions such as ARVs can induce metabolic stress, skewing the cell's immune response and restricting (cell) growth. Novel metabolomic techniques provided the opportunity to investigate the impact of fetal HIV-1 and combination ARV therapy (cART) exposure on the infants' immune metabolome. Peroxidized lipids, generated by reactive oxygen species, were increased in cART/HIV-1–exposed infants, indicating altered mitochondrial functioning. The lipid metabolism was further dysregulated with increased triglyceride species and a subsequent decrease in phospholipids in cART/HIV-1–exposed infants compared to control infants. Proinflammatory immune mediators, lysophospholipids as well as cytokines such as CXCL10 and CCL3, were increased whereas anti-inflammatory metabolites from the cytochrome P450 pathway were reduced in cART/HIV-1–exposed infants. Taken together, these data demonstrate that the fetal metabolism is impacted by maternal factors (cART and HIV-1) and skews physiological immune responses toward inflammation in the newborn infant.

**Keywords.** immune metabolism; fetal development; HIV-1; metabolomics; antiretroviral therapy.

Although the global rollout of antiretroviral (ARV) treatment to prevent mother-to-child transmission of human immunodeficiency virus type 1 (HIV-1) has dramatically improved survival of the 1.4 million infants born annually to HIV-1–infected women [1], increased morbidity is still reported [2, 3]. Studies have shown in utero growth restriction, altered cardiac functioning, and enhanced susceptibility to infections in children born to HIV-1–infected women [2, 4–6]. Furthermore, there are concerns regarding neurological abnormalities in combination ARV therapy (cART)/HIV-1–exposed infants [7, 8]. In

addition, immune responses from both the innate as well as the adaptive arm of the immune system are altered in cART/HIV-1–exposed infants [9–11]. The underlying mechanisms responsible for these clinical and immunological observations remain largely unknown, in particular as even infants born to immune-competent women receiving cART with an undetectable viral load still present with immune alterations [10].

During infections but also through pharmacological interventions, metabolic stress impacts the cell's immune response. Changes in nutrient levels are sensed by nutrient-sensing (stress) receptors in the endoplasmic reticulum (ER) [12], which activate the unfolded-protein response [12] and subsequent nuclear factor kappa-light-chain-enhancer of activated B cells (NF- $\kappa$ B) and the c-Jun N-terminal kinase (JNK) pathways [13]. Furthermore, reactive oxygen species (ROS) generated upon mitochondrial stress are potent inducers of the inflammasome and interleukin (IL) 1 $\beta$  production [14]. Pregnancy is a condition of extreme nutrient consumption and places stringent demands on the maternal and fetal metabolism [15]. When nutrient levels are impaired, for example, in children with restricted in utero growth, proinflammatory cytokines in placenta are increased [16, 17], suggesting an immune-metabolic link.

Furthermore, ARVs such as zidovudine, which is frequently used in prevention of mother-to-child transmission (PMTCT)

Received 1 February 2017; editorial decision 9 June 2017; accepted 15 June 2017; published online June 17, 2017.

Presented in part: Nederlandse Organisatie voor Wetenschappelijk Onderzoek (NWO) meeting, Chemistry as Innovating Science (CHAINS), Veldhoven, The Netherlands, 08 December 2016.

Present affiliation: <sup>a</sup>Johnson & Johnson Pharma R&D, Beerse, Belgium. <sup>b</sup>T. H. and M. J. B. contributed equally to this work.

Correspondence: M. J. Bunders, MD, PhD, M01-118, Academic Medical Center (AMC), Meibergdreef 11, 1100AZ Amsterdam, The Netherlands (m.j.bunders@amc.uva.nl).

The Journal of Infectious Diseases® 2017;216:436–46

© The Author 2017. Published by Oxford University Press for the Infectious Diseases Society of America. This is an Open Access article distributed under the terms of the Creative Commons Attribution-NonCommercial-NoDerivs licence (<http://creativecommons.org/licenses/by-nc-nd/4.0/>), which permits non-commercial reproduction and distribution of the work, in any medium, provided the original work is not altered or transformed in any way, and that the work is properly cited. For commercial re-use, please contact [journals.permissions@oup.com](mailto:journals.permissions@oup.com). DOI: 10.1093/infdis/jix291

HIV-1 regimens, reduce the DNA polymerase in mitochondria and can lead to mitochondrial stress [18]. In cART/HIV-1–exposed infants, altered levels of mitochondrial DNA as well as acyl-carnitine profiles have been detected, indicating that mitochondrial functioning may be impaired in these infants [8, 19–23]. We hypothesized that metabolic homeostasis is disrupted in infants exposed in utero to maternal HIV-1 infection and cART, which results in proinflammatory fetal immune responses. Using novel metabolomic techniques, we detected extensive lipid and mitochondrial dysregulation in cord blood–derived plasma of cART/HIV-1–exposed infants compared with HIV-1–unexposed control infants, which was associated with a differential increase of proinflammatory cytokines. These results reveal potential mechanisms by which metabolic processes can shape the fetal immune system, providing the underlying conditions for proinflammatory responses.

## METHODS

### Patients

Plasma was obtained from cord blood collected from 12 infants born to HIV-1–infected women and from 15 control infants born to HIV-1–negative mothers (and not exposed to cART). The required sample size was informed by previously published work in patas monkeys as well as in cART/HIV-1–exposed infants [24, 25]. The samples were collected at the Academic Medical Center (Amsterdam, the Netherlands). The study was approved by the local ethics committee and informed consent was obtained from participating mothers. For the cART/HIV-1–exposed group, maternal viral load, CD4<sup>+</sup> T-cell count, total triglyceride and total cholesterol levels, and antiretroviral medications were obtained from the patient hospital records (Supplementary Table 1). Total triglyceride and total cholesterol levels were not available for the control group. The cART regimen that was used for each patient (Supplementary Table 1) was based on viral resistance or the patient’s treatment regimen prior to conception. Per European guidelines, the cART regimen consisted of 2 nucleoside reverse transcriptase inhibitors (NRTIs; primarily zidovudine and lamivudine) and either a protease inhibitor (PI; ritonavir–boosted lopinavir or nelfinavir) or a nonnucleoside reverse transcriptase inhibitor (NNRTI; nevirapine) [26]. Five of the 12 women were receiving cART treatment prior to pregnancy. One patient took tenofovir during the first trimester of pregnancy combined with lamivudine and nevirapine, while another received nevirapine (NNRTI), in combination with ritonavir–boosted lopinavir and saquinavir due to her resistance profile. During birth, all HIV-1–infected mothers were given intrapartum zidovudine. The clinical profile at delivery of the 12 mothers in the study indicates that the virus was suppressed appropriately, consistent with a mother-to-child transmission rate of <1%. HIV-1 infection was evaluated at birth, 5 weeks, and 3 months by measuring RNA viral load with polymerase chain reaction and confirmed at 18 months of age,

by showing absence of detectable HIV immunoglobulin G. All infants were confirmed to be HIV-1–negative.

### Sample Collection

Plasma was separated by centrifugation at 5000g for 10 minutes at 4°C and stored at –20°C prior to analysis and transported to the Biomedical Facility Leiden (Leiden University) for metabolomics analysis.

### Quality Control Samples

Quality control (QC) samples were used during the metabolomics analyses. Equal volumes of each study sample were pooled to generate a QC pool. A set of QC samples was then included in the analyses with the experimental groups on the individual metabolomics platforms, and the QC samples were distributed randomly through the samples prior to liquid chromatography–mass spectrometry (LC–MS) analysis. In addition, independent duplicate samples were randomly selected. Only those metabolites for which the duplicate and QC samples had a relative standard deviation <30% were considered to be measured accurately.

### LC–MS Targeted Metabolomics Analyses

Targeted metabolomics analyses were performed using standard operating procedures based on previously published methods [27, 28]. The detailed procedures and target lists are provided in the Supplementary Data (Experimental Procedures).

### Positive and Negative Lipid Profiling

Ten-microliter and 20- $\mu$ L serum samples were spiked with calibration and internal standards and extracted using isopropyl alcohol (for the positive lipid platforms) or methanol (for the negative lipid platforms). Samples were analyzed using an ACQUITY ultra performance liquid chromatography system coupled to a 6530 Accurate Mass Quadrupole time-of-flight (Agilent Technologies, Santa Clara, California) [28].

### Oxylipin Profiling

One hundred fifty-microliter serum samples were spiked with calibration and internal standards and diluted with a 5% methanol solution containing 0.1% acetic acid. Samples were extracted using solid-phase extraction (HLB Oasis, Waters Chromatography) and analyzed using an high performance liquid chromatography system coupled to a 6460 Agilent Triple Quadrupole mass spectrometer (Agilent Technologies) [27].

### Soluble Immunological Factors

A multiparameter Luminex bead assay (Invitrogen) was used to measure the levels of the following soluble factors in 25  $\mu$ L of plasma in accordance with the manufacturer’s instructions: IL-1B, IL-4, IL-5, IL-6, IL-8, IL-10, IL-13, IL-17A, IL-18, interferon (IFN)– $\alpha$ , IFN– $\gamma$ , CXCL10, tumor necrosis factor, CCL3, CCL4, CCL5, TNF-related apoptosis-inducing ligand (TRAIL), and colony stimulating factor 2 (CSF2). Human serum

C-reactive protein was measured with enzyme-linked immunosorbent assay (R&D Systems, Abingdon, United Kingdom).

### Statistical Analyses

A combination of univariate bioinformatics approaches was performed using the R script-based online tool Metaboanalyst 3.0 [29]. Mann–Whitney *U* test and Fisher exact test were used to compare differences in patient demographics on continuous and categorical variables, respectively, using SPSS version 23.0 software (IBM Corp, Armonk, New York). Pearson correlation coefficients were calculated using SPSS. Significant Pearson correlations between immunological markers and metabolites were visualized using the Metscape application within Cytoscape (version 3.2.1) [30].

Following LC-MS analysis, peak integration, and determination of the relative ratios between metabolites and their corresponding internal standards, QC quality assurance was performed. First, we evaluated for outlier samples based on a 95% confidence region in a Hotelling T-squared distribution test. No outlier samples were identified in all the platforms measured. Significant metabolites were identified based on the following 2 criteria: (1) a fold change (FC)  $\geq 1.25$  or  $\leq 0.75$ , indicating a 25% increase or decrease, respectively, and (2) a

*P* value  $< .05$  using the Mann–Whitney *U* test. The significant univariate results are shown on a volcano plot as colored symbols. Pearson correlation coefficients were generated using log-transformed normalized data in SPSS. During the correlation analyses, each metabolite was tested against 8 immunological markers, and no multiple testing correction was performed, as only class responses—and not individual correlations—were interpreted. Significant correlations were defined as a Pearson coefficient (*r*)  $> 0.46$  or  $r < -0.46$  and *P*  $< .05$ .

### RESULTS

In this study, 12 cART-treated HIV-1–infected and 15 HIV-1–negative pregnant women were included. The baseline maternal group demographics (Table 1) were similar, except ethnicity. In HIV-1–infected women, triglyceride (1.8 mmol/L) and total cholesterol (5 mmol/L) levels were within upper-normal ranges for pregnant women [31] and none of the HIV-1–infected women or in the control group had diabetes or were diagnosed with gestational diabetes. The HIV-1–infected women had a CD4<sup>+</sup> T-cell count in the first trimester exceeding  $200 \times 10^6$  cells/L in all women (Table 1). The CD4<sup>+</sup> T-cell counts further increased and viral load decreased after initiating cART; at

**Table 1. Patient Demographics**

Clinical Variables	Control Mothers (n = 15)		HIV-Infected Mothers (n = 12)		P Value
	Median (75% CI)		Median (75% CI)		
Age, y	32.6 (30.7–33.2)		28.5 (28.2–32.4)		.50 <sup>a</sup>
Prepregnancy weight, kg	64.5 <sup>b</sup> (62.7–66.9)		68.5 (65.7–74.2)		.41 <sup>a</sup>
Prepregnancy BMI	22.04 <sup>b</sup> (22.3–24.1)		23.67 (22.6–26.1)		.79 <sup>a</sup>
Total triglycerides <sup>c</sup> , mmol/L	...		1.80 <sup>d</sup> (1.5–2.1)		
Total cholesterol <sup>e</sup> , mmol/L	...		5 <sup>d</sup> (4.6–5.4)		
Glucose <sup>e</sup> , mmol/L	...		4.30 <sup>d</sup> (4.2–4.7)		
Ethnicity (white/black/South Asian), No.	9/4/2		3/9/0		.03 <sup>e</sup>
Gestational diabetes (yes/no), No.	0/15		0/12		
Viral load, copies/mL	Trimester 1	...	528.5 (1269–9084)		
	Trimester 2	...	50 (47.81–281)		
	Trimester 3 <sup>f</sup>	...	<50		
CD4 count, $\times 10^6$ cells/L	Trimester 1	...	455 (465.5–594.5)		
	Trimester 2	...	520 (511.4–650.6)		
	Trimester 3	...	700 (616.5–792.5)		
<hr/>					
	Control Infants (n = 15)		cART/HIV-1–Exposed Infants (n = 12)		
Gestation period, wk	40 (37.63–39.97)		39.25 (38.74–39.82)		.57 <sup>a</sup>
Birth weight, g	3380 (3128–3494)		3085 (3009–3472)		.34 <sup>a</sup>
Apgar score (5 min)	10 (9.5–9.9)		10 (9.1–9.9)		.44 <sup>a</sup>
Mode of delivery (vaginal/cesarean), No.	14/1		8/4		.14 <sup>e</sup>
Gender (male/female), No.	8/7		7/5		.55 <sup>e</sup>

Abbreviations: BMI, body mass index; CI, confidence interval.

<sup>a</sup>Mann–Whitney *U* test.

<sup>b</sup>One missing value.

<sup>c</sup>Measured at the end of the second trimester.

<sup>d</sup>Two missing values.

<sup>e</sup>Fisher exact test.

<sup>f</sup>All mothers were below the limit of detection.

delivery, viral loads were undetectable in all women (Table 1). Five of the 12 women were receiving cART treatment prior to pregnancy. None of the HIV-1-infected mothers transmitted the virus to their infant. The cART/HIV-1-exposed and control infants had a similar distribution with regards to gestational age, birth weight, Apgar scores, mode of delivery, and sex.

#### Oxidative Stress in cART/HIV-1-Exposed Infants

Reactive oxygen species are produced upon mitochondrial dysfunction, in particularly upon cell stress. Therefore, to assess the outcome of mitochondrial dysfunctioning, we measured ROS-catalyzed lipid peroxidation metabolites [32]. Predefined criteria identified 13 significantly increased ROS-produced oxylipins with a 0.25 FC and  $P < .05$  (see Statistical Analyses). Moreover, none of the peroxidized oxylipins were decreased in the cART/HIV-1-exposed infants (Figure 1 and Supplementary Table 2). These findings point toward mitochondrial dysfunctioning in cART/HIV-1-exposed infants, resulting in increased ROS production. ROS are strong activators of lipogenesis, and we therefore next investigated the infants' lipid profiles.

#### Lipid Profiles in cART/HIV-1-Exposed Infants Are Characterized by Hypertriglyceridemia and Decreased Phospholipid Species

We evaluated the effect of in utero cART/HIV-1 exposure on lipid metabolism in infants by measuring their triglyceride,

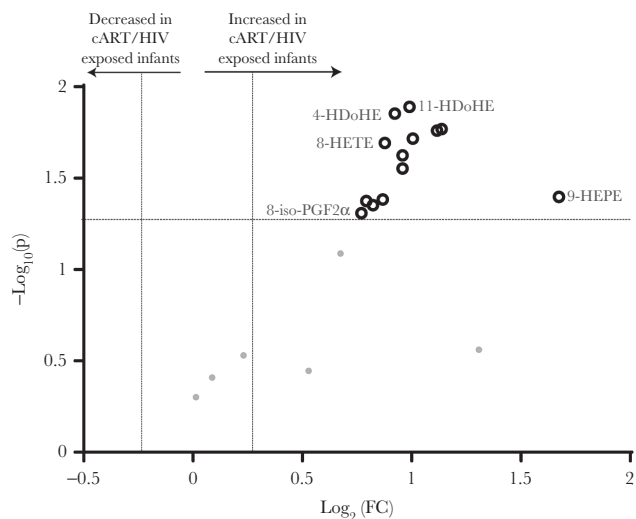


**Figure 1.** Volcano plot of the reactive oxygen species–produced oxylipin profiles of combination antiretroviral therapy (cART)/human immunodeficiency virus type 1 (HIV-1)–exposed infants vs control infants. Thirteen metabolites were identified as significantly increased (black rings) in the cART/HIV-1-exposed-infants compared to control infants. Volcano plots visualizes the  $\log_{10}$  (Mann–Whitney  $P$  value) on the y-axis and the  $\log_2$  (fold change [FC]) on the x-axis for each metabolite compared between the cART/HIV-1-exposed infants vs control infants. The dotted lines represent the significance thresholds with  $FC > 1.25$  and  $FC < 0.75$  on the x-axis and  $P < .05$  on the y-axis. Abbreviations: 8-iso-PGF $_2\alpha$ , 8-iso-prostaglandin  $F_2\alpha$ ; cART, combination antiretroviral therapy; FC, fold change; HDoHE, hydroxyl-docosahexaenoic acid; HEPE, hydroxy-eicosapentaenoic acid; HETE, hydroxy-eicosatetraenoic acid; HIV, human immunodeficiency virus.

diacylglycerol, sphingomyelin, phospholipid, cholesteryl ester, and free fatty acid cord blood profiles. Free fatty acids are the simplest lipid metabolites, with the phospholipids containing 2 free fatty acids bound to a glycerol phosphate backbone. Phospholipids are critical building blocks in cell and organelle membrane structure, function and integrity, with their metabolism regulated by the different phospholipases. Similarly, the diacylglycerol (triglyceride precursors) and triglycerides metabolites are important in free fatty acid storage acting as an energy reservoir, and have a lesser role in membrane structure and signaling (diacylglycerols). The sphingomyelins are members of the unique sphingolipids and play an important role in the central nervous system, as well as in lipid rafts (together with cholesterol). In total, 2 diacylglycerols and 32 triglycerides were increased. In particularly, triglycerides with long and very long acyl chains were significantly increased in cART/HIV-1-exposed infants. As only free fatty acids are transported across the placenta to the fetus [33], and no differences in free fatty acids between cART/HIV-1-exposed infants and control infants were detected, these increased triglyceride levels in the infant depend on nonspecific fatty acid elongation and endogenous triglyceride biosynthesis. Although not yet described in cART/HIV-1-exposed infants, hypertriglyceridemia is commonly observed in HIV-1-infected adults, in particular, in patients treated with ritonavir-boosted lopinavir, to which 8 of 12 infants were exposed [34]. Triglyceride synthesis occurs primarily in the endoplasmic reticulum (ER). To remove the surplus of triglycerides from the ER, the ER commences the formation of lipid droplets with an outer rim of ER membrane-derived phospholipids. We therefore evaluated phosphatidylcholines and phosphatidylethanolamines, which are the most prevalent glycerophospholipids and components of the ER membrane. Three phosphatidylcholines, 2 plasmalogen phosphatidylcholines, and 1 phosphatidylethanolamine metabolite were significantly decreased in cART/HIV-1-exposed infants compared to control infants (Figure 2 and Supplementary Table 2). Depletion of ER membrane-derived phospholipids upon hypertriglyceridemia is an important ER stressor. In addition, phospholipids—and specifically unsaturated lysophospholipids—have anti-inflammatory properties, inhibiting NF- $\kappa$ B activation via the mitogen-activated protein kinase pathway [35], whereas saturated lysophospholipids have a proinflammatory effect. We subsequently assessed the lysophospholipids in both cART- and HIV-exposed infants and controls. Of note, no differences were detected in the cholesteryl ester profiles, whereas 2 sphingomyelin species were decreased in the cART/HIV-1-exposed infants compared to the controls.

#### Increased Saturated and Decreased Unsaturated Lysophospholipids in cART/HIV-1-Exposed Infants

Lysophospholipids are derived from the phospholipases-mediated hydrolyses of 1 of the 2 (SN $_1$  or SN $_2$  position) acyl chains



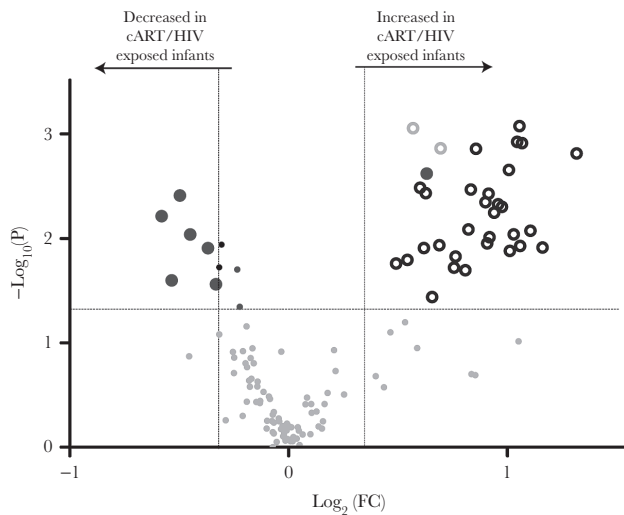


**Figure 2.** Volcano plot of lipid profiles of combination antiretroviral therapy (cART)/ human immunodeficiency virus type 1 (HIV-1)-exposed infants vs control infants. Overall, 32 triglycerides (black rings) and 2 diacylglycerols (gray rings) were increased with 6 phospholipids (large dark grey circles) having decreased levels in cART/HIV-1-exposed infants compared to control infants. Sphingomyelins (black dots) and phospholipids (small dark grey dot) with  $P < .05$  are also shown. Volcano plots visualizes the  $\log_{10}$  (Mann-Whitney  $P$  value) on the y-axis and the  $\log_2$  (fold change [FC]) on the x-axis for each metabolite compared between the cART/HIV-1-exposed infants vs control infants. The dotted lines represent the significance thresholds with  $FC > 1.25$  and  $FC < 0.75$  on the x-axis and  $P < .05$  on the y-axis.

in the phospholipids, resulting in a lysophospholipid (fatty acid bound to the phospho-glycerol backbone) and a free fatty acid. Lysophospholipids released into the circulation, function as immune modulators and fatty acid transporters. Two saturated stearic acid isomers ( $SN_1$ -lysophosphatidylcholine C18:0 and  $SN_2$ -lysophosphatidylcholine C18:0) and 2 saturated lysophosphatidylethanolamine species (C16:0 and C18:0) were significantly increased in cART/HIV-1-exposed infants compared to control infants (Figure 3A and Supplementary Table 2). The unsaturated  $\omega$ -9  $SN_1$ -lysophosphatidylcholine C20:3 was reduced in cART/HIV-1-exposed infants compared to control infants. The ratios of saturated vs unsaturated lysophosphatidylcholines and lysophosphatidylethanolamines were significantly ( $P < .01$ ) increased in the cART/HIV-1-exposed infants compared to the control infants due to increased saturated lysophospholipids species (Figure 3B). In contrast, this ratio was balanced in the control group, indicating that unexposed infants maintain homeostatic control.

#### Anti-Inflammatory Oxylipin Mediators Are Decreased in cART/HIV-1-Exposed Infants

Like lysophospholipids, the oxylipins are enzymatically synthesized from the free fatty acids produced by enzyme-mediated hydrolysis of membrane phospholipids in 3 major pathways. First, free fatty acids can follow the cyclooxygenase-II (COX) pathway, leading to well-known prostaglandins

or thromboxanes [36]. COX pathway metabolites are critical in inflammatory responses during infection and are common targets for therapeutic interventions [36]. Free fatty acids can be also oxidized by cytochrome P450 (CYP450) enzymes resulting in the epoxy-fatty acid oxylipins, which play a predominantly anti-inflammatory role [37]. Last, the third oxidation pathway is the 5-,12- and 15-lipoxygenase (LOX) pathway. Important downstream metabolites of the LOX pathway are hydroxy-fatty acids and leukotrienes, which play a role in inflammation, for example in asthma [36]. The CYP450 oxylipins 5,6-dihydroxyeicosatrienoic acid (DiHETre), 8,9-DiHETre, and 11,12-DiHETre were significantly reduced in the cART/HIV-1-exposed infants, indicating impaired CYP450 metabolism in this group (Figure 4 and Supplementary Table 2). Interestingly, 11,12-epoxyeicosatrienoic acid, which was significantly reduced in cART/HIV-1-exposed infants compared to control infants, is a potent inhibitor of the NF- $\kappa$ B pathway [38]. Epoxyeicosatrienoic acids also activate PPAR $\alpha$ , which in turn induces mitochondrial  $\beta$ -oxidation as well as regulates the secretion of insulin and glucagon, thereby acting as antihyperlipidemia and antihyperglycemia agents [39]. The reduction in DiHETre levels therefore indicates a reduced antihyperlipidemia capacity in cART/HIV-1-exposed infants.

The other 4 identified enzyme-derived oxylipin metabolites are in the LOX pathway and included 20-carboxy-leukotriene  $B_4$ , protectin DX (PDX), 5-hydroxyeicosapentaenoic acid (5-HEPE), and 9-hydroxyoctadecatrienoic acid (9-HOTre). Notably, 20-carboxy-leukotriene  $B_4$ , which was increased in cART/HIV-1-exposed infants, is the stable downstream metabolite of leukotriene  $B_4$ , a potent proinflammatory mediator in asthma. Overall, the changes in oxylipin levels measured in cART/HIV-1-exposed infants indicate a skewing toward metabolites with proinflammatory capacity while compensatory mechanisms are reduced.

#### Dyslipidemia and Peroxidized Lipids Indicating Mitochondrial Dysfunction Are Associated With Increased Proinflammatory Cytokines and Chemokines in cART/HIV-1-Exposed Infants

To determine associations between the proinflammatory lipid mediators, cytokines, and chemokines were measured [10]. The levels of IL-4, IL-5, IL-13, IL-17A, IL-18, and IFN- $\alpha$  and IFN- $\gamma$  were below the detection limit, and CRP was  $>3$  log lower than the clinically relevant cutoff (data not shown). Correlations between the metabolites and immune markers were calculated. Figure 5 shows networks for the metabolite classes that correlated significantly to the immunological markers (Supplementary Tables 3–7). ROS-catalyzed lipid peroxidation products correlated strongly with CXCL10 and to a lesser extent to CCL4 (Figure 5A). Triglycerides, diacylglycerols, and phospholipids (Figure 5B) correlated with IL-8, CCL3, and, to a lesser extent, CCL4 and IL-1B. Furthermore, saturated and unsaturated lysophospholipids (Figure 5C) were, respectively, positively and

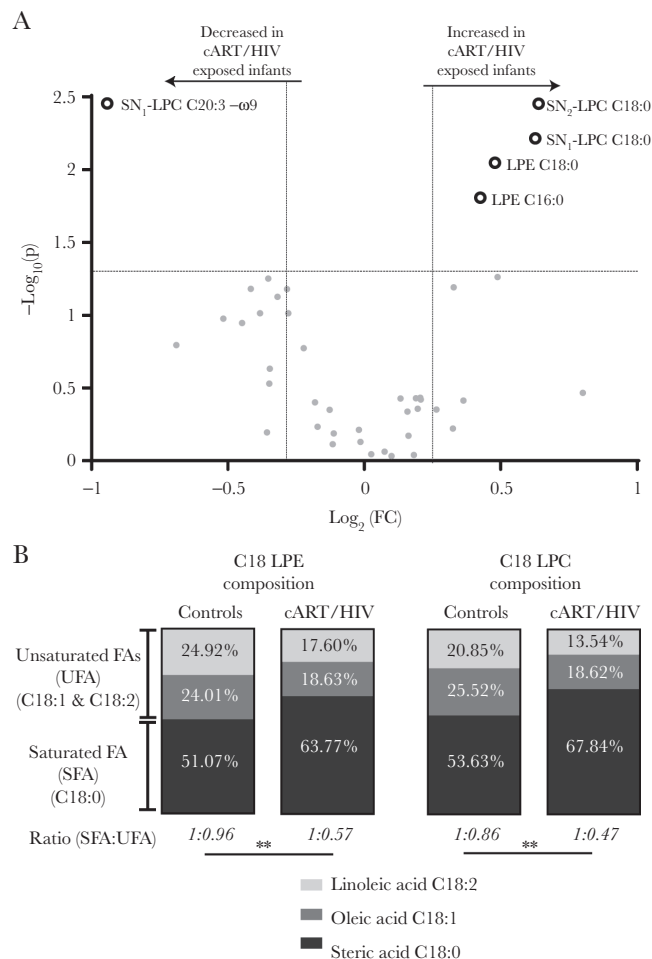


**Figure 3.** The lysophospholipid profiles of combination antiretroviral therapy (cART)/ human immunodeficiency virus type 1 (HIV-1)-exposed infants vs control infants. *A*, Lysophospholipid profiles: The increased saturated lysophospholipids and decreased unsaturated lysophospholipid in the plasma of cART/HIV-1-exposed infants are shown as dark grey rings on the volcano plot. Volcano plots visualizes the  $\log_{10}$  (Mann-Whitney  $P$  value) on the y-axis and the  $\log_2$  (fold change [FC]) on the x-axis for each metabolite compared between the cART/HIV-1-exposed infants vs control infants. The dotted lines represent the significance thresholds with FC  $\geq$  1.25 and FC  $\leq$  0.75 on the x-axis and  $P < .05$  on the y-axis. *B*, Lysophospholipid saturation composition average: a significant change in the ratio of saturated vs unsaturated C18 lysophosphatidylethanolamine and lysophosphatidylcholine species was found in the cART/HIV-1-exposed infants compared to control infants. Ratios revealed an almost doubling in the percentage of stearic acid vs oleic and linoleic acid species in cART/HIV-1-exposed infants. Black, gray, and light gray represents the group-averaged stearic acid (C18:0), oleic acid (C18:1), and linoleic acid (C18:2), respectively. Unpaired  $t$  test on the intergroup ratios. **\*\*** $P < .01$ . Abbreviations: cART, combination antiretroviral therapy; FA, fatty acid; FC, fold change; HIV, human immunodeficiency virus; LPC, lysophosphatidylcholine; LPE, lysophosphatidylethanolamine; SFA, saturated fatty acid; SN, stereospecific numbering; UFA, unsaturated fatty acid.

negatively associated with CCL3, CCL4, and CXCL10. Products from the LOX and COX pathways were positively associated with IL-1B, IL-8, CCL3, CCL4, and CXCL10 (Figure 5D). Together, these studies show an accumulation of proinflammatory metabolite mediators such as saturated lysophospholipids, triglycerides, and lipid peroxidation metabolites, which were associated with proinflammatory cytokines and chemokines.

## DISCUSSION

Using comprehensive and highly sensitive metabolomics tools, we demonstrate that the metabolome in infants exposed to long-term cART in utero is characterized by cell stress and dysregulation of metabolites with immune modulatory capacities in cART/HIV-1-exposed infants. These studies further suggest

that physiologic metabolic functioning during fetal development is critical for maintaining a tolerant immune milieu. When metabolic homeostasis is disrupted and cell stress is induced either by viruses or pharmacological interventions, the tolerant fetal immune system can be skewed toward proinflammatory immune responses, with potential consequences for pregnancy outcome and postnatal immune competence.

The augmented peroxidized lipids provide a robust indication of the in vivo consequences of altered mitochondrial functioning in cART/HIV-1-exposed infants. As these children are not infected with HIV-1 and zidovudine is actively transported across the placenta [40], the altered mitochondrial functioning in cART/HIV-1-exposed infants is likely due to the effects of zidovudine on the mitochondrial DNA polymerase and the

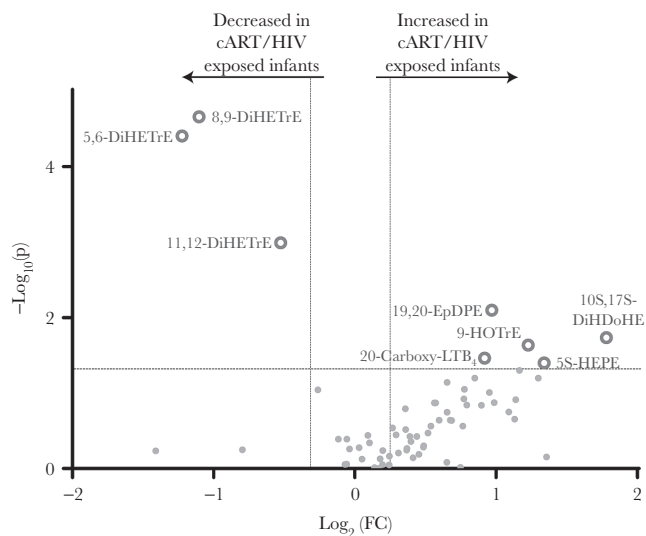


**Figure 4.** Volcano plot of cyclooxygenase, lipoxygenase, and cytochrome P450 oxylipin profiles of combination antiretroviral therapy (cART)/human immunodeficiency virus type 1 (HIV-1)-exposed infants vs control infants. Significantly increased or decreased oxylipins in the cART/HIV-1-exposed-infants compared to the control infants are shown as grey rings. Volcano plots visualizes the  $\log_{10}$  (Mann-Whitney  $P$  value) on the y-axis and the  $\log_2$  (fold change [FC]) on the x-axis for each metabolite compared between the cART/HIV-1-exposed infants vs control infants. The dotted lines represent the significance thresholds with  $FC > 1.25$  and  $FC < 0.75$  on the x-axis and  $P < .05$  on the y-axis. Abbreviations: 20-carboxy-LTB<sub>4</sub>, 20-carboxy-leukotriene B<sub>4</sub>; cART, combination antiretroviral therapy; DiHDoHE, dihydrodocosa-4,7,11,13,15,19-hexaenoic acid; DiHETrE, dihydroxy-eicosatrienoic acid; EpDPE, epoxy-docosapentaenoic acid; FC, fold change; HEPE, hydroxy-eicosapentaenoic acid; HIV, human immunodeficiency virus; HOTrE, hydroxy-9Z,11E,15Z-octadecatrienoic acid.

electron transport chain's complexes assembling. Interestingly, the 1 infant without in utero NRTI exposure had a lipid peroxidation metabolite profile comparable to those of the control infants. None of the infants presented with lipodystrophy; however, exposure time was also shorter than when lipodystrophy is generally clinically visible in cART-treated patients. The consequences of mitochondrial toxicity may persist after exposure has ceased as studies in patas monkeys showed abnormal cardiac mitochondrial morphology at 1 year and aneuploidy persisting for up to 3 years of age [41, 42]. Furthermore, a recent study by Jao et al showed that the acyl-carnitine profile and branched amino acids were associated with an altered insulin metabolism in cART/HIV-1-exposed infants at 6 weeks of age [43]. Together, these observations underscore the need for studies assessing whether changes in the fetal metabolism resulting from exposure to ARV have long-term clinical consequences. Furthermore, ARVs with reduced toxicity compared to zidovudine are available and used in the setting of treatment of HIV-1-infected adults and children as well as PMTCT. The avoidance of zidovudine in PMTCT regimens is now a realistic option to prevent zidovudine-associated metabolic dysregulation.

Significant changes were further detected in the lipid metabolism in cART/HIV-1-exposed infants. Birth is a metabolic

stressful period for both mother and infant, with little recent food intake. Therefore, significant changes of metabolites reflect metabolic functioning and less likely of differences in food intake between HIV-1-infected mothers and controls. Increased triglycerides are a well-known phenomenon in HIV-1-infected patients and have been attributed to several causes, including increased type 1 interferons, microbial translocation, and several antiretroviral drugs [34, 44]. Of these, PIs are most notorious in inducing hypertriglyceridemia. The reduced levels of CYP4A and CYP2B6 eicosanoids in cART/HIV-1-exposed infants support a direct effect of PIs on fetal cells, as PIs have been shown to inhibit CYP450 enzyme activity [45]. After cessation of PI treatment, adults' triglyceride levels return to normal values, suggesting that this may also occur in the cART/HIV-1-exposed infants. However, consequences of the altered lipid metabolism may reach beyond its effect on immune responses. Of note, the increased triglyceride levels in cART/HIV-1-exposed infants may be an underestimate of the impact of in utero HIV-1 and cART exposure, as triglyceride levels in black populations are lower compared to white populations, and more cART/HIV-1-exposed infants were black compared to the control infants [46]. These findings suggest that lopinavir/ritonavir-based regimes might not be the ideal candidate for PMTCT of HIV-1 [47], even as monotherapy. However, darunavir, which has potent antiviral capacity in combination with a more favorable lipid profile, might be a more suitable candidate in cART and is currently also evaluated in the setting of PMTCT as monotherapy [48] (ClinicalTrials.gov identifier NCT02738502). Furthermore, integrase inhibitors may present a less toxic alternative as well for PMTCT.

Our study at the interface of immune and metabolic responses provides new insights in the role of metabolites with immunomodulatory capacities prior to birth. Lipid peroxidation products positively correlated with CXCL10, which is an interferon-stimulated gene. West et al described that in mice with mitochondrial stress, interferon-stimulated genes were upregulated [49]. Additionally, hypertriglyceridemia can activate the ER stress's unfolded protein response and downstream proinflammatory pathways. Last, significantly lower levels of the potent anti-inflammatory arachidonic acid-derived CYP450 metabolites were detected in the cART/HIV-1-exposed infants, reducing compensatory homeostatic mechanisms in these infants. Further studies are required to understand how these changes in metabolites and associated immune responses indicating low-level inflammation provide the underlying conditions for the described morbidity such as increased susceptibility to infections of cART/HIV-1-exposed infants [2, 3, 21]. Although enhanced immune activation may seem at odds with increased susceptibility to infections, the continuous low-level immune activation in, for example, obese patients has been proposed to contribute to enhanced susceptibility to infections [50]. The immunometabolic prolife of

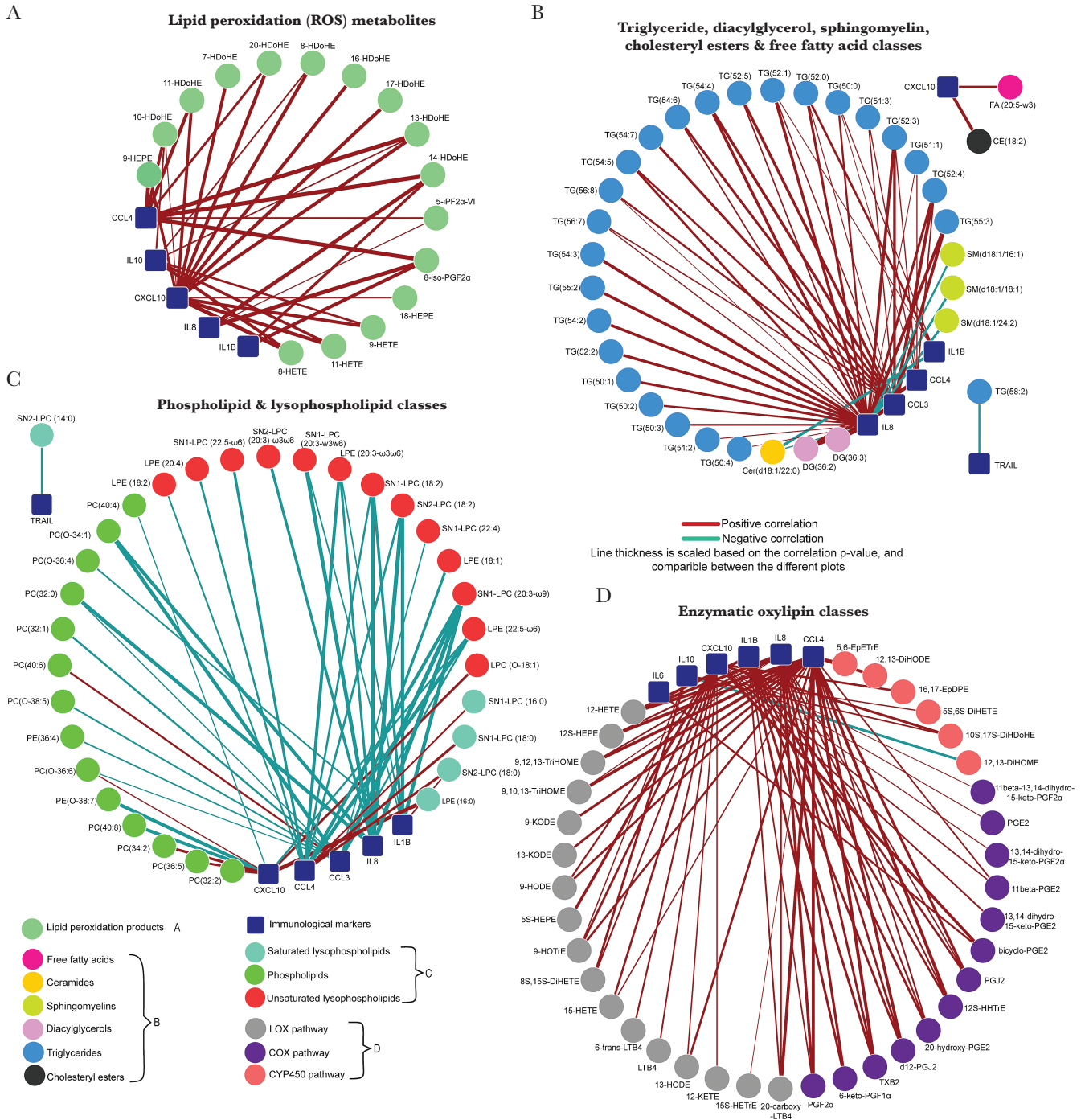


**Figure 5.** Pearson correlation networks illustrating the correlation between metabolite classes and classic immunological markers. The correlation network shows the correlations ( $P < .05$ ) between the measured cytokines and chemokines and the normalized metabolites for reactive oxygen species lipid peroxidation metabolites (A); triglycerides, sphingomyelins, diacylglycerols, cholesteryl esters, and free fatty acids (B); phospholipids and lysophospholipids (C); and enzymatic oxylipins (D) (Supplementary Tables 3–7). Abbreviations: 5-iPGF2 $\alpha$ -VI, 5-isoprostane F2 $\alpha$  VI; 8-iso-PGF2 $\alpha$ , 8-iso-prostaglandin F2 $\alpha$ ; CE, cholesteryl ester; Cer, ceramides; COX, cyclooxygenase; CYP450, cytochrome P450; DG, diacylglycerol; DiHDoHE, dihydroxydocosahexaenoic acid; DiHETE, dihydroxyeicosatetraenoic acid; DiHETrE, dihydroxyeicosatrienoic acid; DiHODE, dihydroxyoctadecadienoic acid; DiHOME, dihydroxyoctadecenoic acid; EpDPE, epoxydocosapentaenoic acid; EpETrE, epoxy-eicosatrienoic acid; FA, free fatty acids; HDoHE, hydroxy-docosahexaenoic acid; HETE, hydroxyeicosatetraenoic acid; HETrE, hydroxyeicosatrienoic acid; HEPE, hydroxyeicosapentaenoic acid; HHTrE, hydroxyheptadecatrienoic acid; HODE, hydroxyoctadecadienoic acid; HOTrE, hydroxy-9Z,11E,15Z-octadecatrienoic acid; KETE, oxo-eicosatetraenoic acid; KETE, oxo-octadecadienoic acid; LPC, lysophosphatidylcholine; LPC(O), plasmalogen lysophosphatidylcholine; LPE, lysophosphatidylethanolamine; LOX, lipoxygenase; LT, leukotriene; PC, phosphatidylcholine; PC(O), plasmalogen phosphatidylcholine; PE, phosphatidylethanolamine; PE(O), plasmalogen phosphatidylethanolamine; PG, prostaglandin; SM – sphingomyelins; SN, stereospecific position; TG, triglyceride; Trail, TNF-related apoptosis-inducing ligand; TriHOME, trihydroxy-octadecenoic acid; TX, thromboxane.



cART/HIV-1–exposed infants partially resembles this phenotype and could contribute to the clinical observations.

Next to avoidance of more toxic regimens, interventions including antioxidants and carnitines could be explored to restore homeostasis and ameliorate immunometabolic dysregulation in HIV-1–infected women and their infants in settings where alternatives are not available. Furthermore, when investigating alternative PMTCT regimens, highly sensitive novel omics approaches such as metabolomics techniques used here, but also transcriptomics or epigenetic analyses, provide a unique opportunity to identify biomarkers in the context of prenatal exposure to ARVs and HIV-1. These techniques would provide a powerful tool to complement pharmacokinetics studies in clinical trials. Studies investigating adverse effects of prenatal exposure of ARVs can be further strengthened by investigating paired prenatal maternal samples and longitudinal infant samples.

In conclusion, our results demonstrate dysregulation of several metabolic pathways in infants with in utero exposure to cART and HIV-1, providing the underlying conditions for a proinflammatory milieu observed in these infants. These data represent a novel framework in which metabolic dysregulation in the fetus is critical in shaping the earliest human immune responses, with potential consequences for fetal development and immunocompetence in the infant.

#### Supplementary Data

Supplementary materials are available at *The Journal of Infectious Diseases* online. Consisting of data provided by the authors to benefit the reader, the posted materials are not copyedited and are the sole responsibility of the authors, so questions or comments should be addressed to the corresponding author.

#### Notes

**Author contributions.** M. J. B. and T. H. served as principal investigators and conceived and designed the study. E. v. L. provided care for the pregnant women and H. J. S. for the infants. J. C. S. and A. C. H. performed the experiments. T. W. K., M. J. B., and G. P. M., E. v. L. and H. J. S. assisted in acquisition of the samples and clinical data. R. B., T. H., R. J. V., and C. J. R. contributed to study design. J. C. S. performed the analyses. J. C. S. and M. J. B. wrote the first draft of the manuscript with input from all authors. All authors approved the final manuscript revisions.

**Acknowledgments.** We thank the women for participating in the study; K. Boer, M. Godfried, and J. Nellen for care of the pregnant women; K. Boer for collection of the samples; J. Fu and V. V. Koval for help with statistical data analyses; the technical staff at the Netherlands Metabolomics Center (NMC) (Leiden University) for metabolomics platform sample analyses and data processing; and A. Drewniak, M. Janssen, and J. van Hamme for help with the immunological assays. All metabolomics data are available in the online MetaboLights data

repository under the accession number MTBLS449 (<http://www.ebi.ac.uk/metabolights/>).

**Financial support.** This work was supported by the Nederlandse Organisatie voor Wetenschappelijk Onderzoek (NWO)-Zon Mw (grant number 435002027) and the Virgo consortium, which is funded by the Dutch government (project number FES0908). Further support was obtained from the Netherlands Organisation for Scientific Research Agiko Stipendium (grant number 92003417) and the Dutch AIDS Foundation (grant number 2006015).

**Potential conflicts of interest.** All authors: No reported conflicts of interest. All authors have submitted the ICMJE Form for Disclosure of Potential Conflicts of Interest. Conflicts that the editors consider relevant to the content of the manuscript have been disclosed.

#### References

1. Townsend CL, Cortina-Borja M, Peckham CS, Ruiter A de, Lyall H, Tookey PA. Low rates of mother-to-child transmission of HIV following effective pregnancy interventions in the United Kingdom and Ireland, 2000–2006. *AIDS* **2008**; 22:973–81.
2. Mollendorf C von, Gottberg A von, Tempia S, et al. Increased risk and mortality of invasive pneumococcal disease in HIV-exposed-uninfected infants <1 year of age in South Africa, 2009–2013. *Clin Infect Dis* **2015**; 60:1346–56.
3. Adler C, Haelterman E, Barlow P, Marchant A, Levy J, Goetghebuer T. Severe infections in HIV-exposed uninfected infants born in a European country. *PLoS One* **2015**; 10:e0135375.
4. Lipshultz SE, Williams PL, Zeldow B, et al. Cardiac effects of in-utero exposure to antiretroviral therapy in HIV-uninfected children born to HIV-infected mothers. *AIDS* **2015**; 29:91–100.
5. Jao J, Abrams EJ. Metabolic complications of in utero maternal HIV and antiretroviral exposure in HIV-exposed infants. *Pediatr Infect Dis J* **2014**; 33:734–40.
6. Sofeu CL, Warszawski J, Ateba Ndongo F, et al. Low birth weight in perinatally HIV-exposed uninfected infants: observations in urban settings in Cameroon. *PLoS One* **2014**; 9:e93554.
7. Tran LT, Roos A, Fouche JP, et al. White matter microstructural integrity and neurobehavioral outcome of HIV-exposed uninfected neonates. *Medicine (Baltimore)* **2016**; 95:e2577.
8. Blanche S, Tardieu M, Rustin P, et al. Persistent mitochondrial dysfunction and perinatal exposure to antiretroviral nucleoside analogues. *Lancet* **1999**; 354:1084–9.
9. Borges-Almeida E, Milanez HMBPM, Vilela MMS, et al; BioMed Central Ltd. The impact of maternal HIV infection on cord blood lymphocyte subsets and cytokine profile in

- exposed non-infected newborns. *BMC Infect Dis* **2011**; 11:38.
10. Bunders MJ, Hamme JL van, Jansen MH, Boer K, Kootstra NA, Kuijpers TW. Fetal exposure to HIV-1 alters chemokine receptor expression by CD4+T cells and increases susceptibility to HIV-1. *Sci Rep* **2014**; 4:6690.
  11. Bunders MJ, Cortina-Borja M, Thorne C, Kuijpers T, Newell M-L. Levels and patterns of neutrophil cell counts over the first 8 years of life in children of HIV-1-infected mothers. *AIDS* **2004**; 18:2009–17.
  12. Efeyan A, Comb WC, Sabatini DM. Nutrient-sensing mechanisms and pathways. *Nature* **2015**; 517:302–10.
  13. Walter P, Ron D. The unfolded protein response: from stress pathway to homeostatic regulation. *Science* **2011**; 334:1081–6.
  14. Harijith A, Ebenezer DL, Natarajan V. Reactive oxygen species at the crossroads of inflammasome and inflammation. *Front Physiol* **2014**; 5:352.
  15. Hadden DR, McLaughlin C; Normal and abnormal maternal metabolism during pregnancy. *Semin Fetal Neonatal Med* **2009**; 14:66–71.
  16. Hahn-Zoric M, Hagberg H, Kjellmer I, Ellis J, Wennergren M, Hanson LA. Aberrations in placental cytokine mRNA related to intrauterine growth retardation. *Pediatr Res* **2002**; 51:201–6.
  17. Raghupathy R, Al-Azemi M, Azizieh F. Intrauterine growth restriction: cytokine profiles of trophoblast antigen-stimulated maternal lymphocytes. *Clin Dev Immunol* **2012**; 2012:734865.
  18. Walker UA, Lebrecht D, Reichard W, et al. Zidovudine induces visceral mitochondrial toxicity and intra-abdominal fat gain in a rodent model of lipodystrophy. *Antivir Ther* **2014**; 19:783–92.
  19. Hernández S, Morén C, López M, et al. Perinatal outcomes, mitochondrial toxicity and apoptosis in HIV-treated pregnant women and in-utero-exposed newborn. *AIDS* **2012**; 26:419–28.
  20. Divi RL, Walker VE, Wade NA, et al. Mitochondrial damage and DNA depletion in cord blood and umbilical cord from infants exposed in utero to Combivir. *AIDS* **2004**; 18:1013–21.
  21. Barret B, Tardieu M, Rustin P, et al. Persistent mitochondrial dysfunction in HIV-1-exposed but uninfected infants: clinical screening in a large prospective cohort. *AIDS* **2003**; 17:1769–85.
  22. Kirmse B, Hobbs CV, Peter I, et al. Abnormal newborn screens and acylcarnitines in HIV-exposed and ARV-exposed infants. *Pediatr Infect Dis J* **2013**; 32:146–50.
  23. Morén C, Noguera-Julián A, Garrabou G, et al. Mitochondrial disturbances in HIV pregnancies. *AIDS* **2015**; 29:5–12.
  24. Olivero OA, Torres LR, Gorjifard S, et al. Perinatal exposure of patas monkeys to antiretroviral nucleoside reverse-transcriptase inhibitors induces genotoxicity persistent for up to 3 years of age. *J Infect Dis* **2013**; 208:244–8.
  25. André-Schmutz I, Dal-Cortivo L, Six E, et al. Genotoxic signature in cord blood cells of newborns exposed in utero to a zidovudine-based antiretroviral combination. *J Infect Dis* **2013**; 208:235–43.
  26. Ryom L, Boesecke C, Gisler V, et al. Essentials from the 2015 European AIDS Clinical Society (EACS) guidelines for the treatment of adult HIV-positive persons. *HIV Med* **2016**; 17:83–8.
  27. Strassburg K, Huijbrechts AML, Kortekaas KA, et al. Quantitative profiling of oxylipins through comprehensive LC-MS/MS analysis: application in cardiac surgery. *Anal Bioanal Chem* **2012**; 404:1413–26.
  28. Hu C, Dommelen J van, Heijden R van der, et al. RPLC-ion-trap-FTMS method for lipid profiling of plasma: method validation and application to p53 mutant mouse model. *J Proteome Res* **2008**; 7:4982–91.
  29. Xia J, Sinelnikov IV, Han B, Wishart DS. MetaboAnalyst 3.0—making metabolomics more meaningful. *Nucleic Acids Res* **2015**; 43:W251–W257.
  30. Shannon P, Markiel A, Ozier O, et al. Cytoscape: a software environment for integrated models of biomolecular interaction networks. *Genome Res* **2003**; 13:2498–504.
  31. Diareme M, Karkalousos P, Theodoropoulos G, Strouzas S, Lazanas N. Lipid profile of healthy women during normal pregnancy. *J Med Biochem* **2009**; 28:152–60.
  32. Kirkinezos IG, Moraes CT. Reactive oxygen species and mitochondrial diseases. *Semin Cell Dev Biol* **2001**; 12:449–57.
  33. Cetin I, Parisi F, Berti C, Mandò C, Desoye G. Placental fatty acid transport in maternal obesity. *J Dev Orig Health Dis* **2012**; 3:409–14.
  34. Zha BS, Wan X, Zhang X, et al. HIV protease inhibitors disrupt lipid metabolism by activating endoplasmic reticulum stress and inhibiting autophagy activity in adipocytes. *PLoS One* **2013**; 8:1–16.
  35. Hartmann P, Szabó A, Eros G, et al. Anti-inflammatory effects of phosphatidylcholine in neutrophil leukocyte-dependent acute arthritis in rats. *Eur J Pharmacol* **2009**; 622:58–64.
  36. Buczynski MW, Dumlao DS, Dennis EA. Thematic review series: proteomics. An integrated omics analysis of eicosanoid biology. *J Lipid Res* **2009**; 50:1015–38.
  37. Larsen BT, Campbell WB, Gutterman DD. Beyond vasodilatation: non-vasomotor roles of epoxyeicosatrienoic acids in the cardiovascular system. *Trends Pharmacol Sci* **2007**; 28:32–8.

38. Node K, Huo Y, Ruan X, et al. Anti-inflammatory properties of cytochrome P450 epoxygenase-derived eicosanoids. *Science* **1999**; 285:1276–9.
39. Ng VY, Huang Y, Reddy LM, Falck JR, Lin ET, Kroetz DL. Cytochrome P450 eicosanoids are activators of peroxisome proliferator-activated receptor alpha. *Drug Metab Dispos* **2007**; 35:1126–34.
40. Treluyer J, Jullien V, Rey E, Fouche M, Firtion G. Maternal-fetal transfer and amniotic fluid accumulation of nucleoside analogue reverse transcriptase inhibitors in human immunodeficiency virus-infected pregnant women. *Society* **2004**; 48:4332–6.
41. Divi RL, Leonard SL, Kuo MM, et al. Cardiac mitochondrial compromise in 1-yr-old *Erythrocebus patas* monkeys perinatally-exposed to nucleoside reverse transcriptase inhibitors. *Cardiovasc Toxicol* **2005**; 5:333–46.
42. Olivero OA, Torres LR, Gorjifard S, et al. Perinatal exposure of patas monkeys to antiretroviral nucleoside reverse-transcriptase inhibitors induces genotoxicity persistent for up to 3 years of age. *J Infect Dis* **2013**; 208:244–8.
43. Jao J, Kirmse B, Yu C, et al. Lower preprandial insulin and altered fuel use in HIV/antiretroviral-exposed infants in Cameroon. *J Clin Endocrinol Metab* **2015**; 100:3260–9.
44. Timmons T, Shen C, Aldrovandi G, et al. Microbial translocation and metabolic and body composition measures in treated and untreated HIV infection. *AIDS Res Hum Retroviruses* **2014**; 30:272–7.
45. Moltke LL von, Greenblatt DJ, Grassi JM, et al. Protease inhibitors as inhibitors of human cytochromes P450: high risk associated with ritonavir. *J Clin Pharmacol* **1998**; 38:106–11.
46. Ellman N, Keswell D, Collins M, Tootla M, Goedecke JH. Ethnic differences in the association between lipid metabolism genes and lipid levels in black and white South African women. *Atherosclerosis* **2015**; 240:311–7.
47. Tubiana R, Mandelbrot L, Chenadec J Le, et al. Lopinavir/ritonavir monotherapy as a nucleoside analogue-sparing strategy to prevent HIV-1 mother-to-child transmission: The ANRS 135 PRIMEVA phase 2/3 randomized trial. *Clin Infect Dis* **2013**; 57:891–902.
48. Arribas JR, Girard P-M, Paton N, et al. Efficacy of protease inhibitor monotherapy vs. triple therapy: meta-analysis of data from 2303 patients in 13 randomized trials. *HIV Med* **2016**; 17:358–67.
49. West AP, Khoury-Hanold W, Staron M, et al. Mitochondrial DNA stress primes the antiviral innate immune response. *Nature* **2015**; 520:553–7.
50. Louie JK, Acosta M, Samuel MC, Schechter R, Vugia DJ, Harriman K. Major article a novel risk factor for a novel virus : obesity and 2009 pandemic influenza A (H1N1). *Clin Infect Dis* **2011**; 52:301–12.